

EUROPEAN ORGANIZATION FOR NUCLEAR RESEARCH

OBSERVATION OF J(3.1) PRODUCTION
IN PROTON-PROTON COLLISIONS
AT THE CERN ISR

F.W. Büsser^{*)}, L. Camilleri, L. Di Lella, B.G. Pope
 and A.M. Smith

CERN, Geneva, Switzerland

B.J. Bluménfeld and S.N. White
 Columbia University, NY, USA^{**)}

A.F. Rothenberg, S.L. Segler and M.J. Tannenbaum
 The Rockefeller University, NY, USA^{†)}

M. Banner, J.B. Chêze, H. Kasha^{††)},
 J.P. Pansart, G. Smadja, J. Teiger, H. Zaccone
 and A. Zylberstejn
 CEN, Saclay, France

MASTER

NOTICE

This report was prepared as an account of work sponsored by the United States Government. Neither the United States nor the United States Energy Research and Development Administration, nor any of their employees, nor any of their contractors, subcontractors, or their employees, makes any warranty, express or implied, or assumes any legal liability or responsibility for the accuracy, completeness or usefulness of any information, apparatus, product or process disclosed, or represents that its use would not infringe privately owned rights.

ABSTRACT

In an experiment performed at the CERN Intersecting Storage Rings (ISR), 11 e^+e^- pairs of high invariant mass value ($> 2.5 \text{ GeV}/c^2$) have been observed. Of these events, 9 can be interpreted as arising from the reaction $p + p \rightarrow J(3.1) + \text{anything}$. The cross-section for this reaction is estimated and compared with the result obtained at lower centre-of-mass energies.

Geneva - 16 June 1975

Submitted to the 1975 International Symposium on
 Lepton and Photon Interactions at High Energies
 Stanford University 21-27 August 1975

^{*)} Permanent address: II. Institut für Experimentalphysik, Hamburg, Germany.

^{**)} Research supported in part by the NSF, USA.

^{†)} Research supported in part by the AEC, USA.

^{††)} Permanent address: Yale University, New Haven, Conn., USA.

DISCLAIMER

This report was prepared as an account of work sponsored by an agency of the United States Government. Neither the United States Government nor any agency Thereof, nor any of their employees, makes any warranty, express or implied, or assumes any legal liability or responsibility for the accuracy, completeness, or usefulness of any information, apparatus, product, or process disclosed, or represents that its use would not infringe privately owned rights. Reference herein to any specific commercial product, process, or service by trade name, trademark, manufacturer, or otherwise does not necessarily constitute or imply its endorsement, recommendation, or favoring by the United States Government or any agency thereof. The views and opinions of authors expressed herein do not necessarily state or reflect those of the United States Government or any agency thereof.

DISCLAIMER

Portions of this document may be illegible in electronic image products. Images are produced from the best available original document.

In the course of an experiment to study high transverse momentum electrons and hadrons at the CERN Intersecting Storage Rings (ISR), evidence has been found for the process

$$p + p \rightarrow e^+ + e^- + \text{anything} \quad (1)$$

occurring for high mass values ($> 2.5 \text{ GeV}/c^2$) of the e^+e^- pairs.

The experimental apparatus, shown in Fig. 1, consisted of two spectrometer arms located around 90° on opposite sides of an ISR intersection region.

Each spectrometer consisted of a system of wire spark chambers with magnetostrictive read-out (labelled SC in Fig. 1), and a magnet with a bending power of $0.343 \text{ T}\cdot\text{m}$, providing a momentum measurement with a standard deviation $\Delta p/p = \sqrt{(0.025)^2 + (0.02p)^2}$ (p in GeV/c).

Electron identification was achieved by means of threshold gas Čerenkov counters and electromagnetic shower detectors. There was one Čerenkov counter in each arm, located in the magnet gap and segmented into eight independent cells. Counter C, belonging to Arm 1, was filled with isobutane (C_4H_{10}) at atmospheric pressure. Counter C', belonging to Arm 2, was filled with air at atmospheric pressure. The corresponding pion momenta at threshold were 2.7 and 5.6 GeV/c , respectively, or 3.1 and 4.9 GeV/c in the centre-of-mass system.

The electromagnetic shower detector in Arm 1 consisted of a 3 radiation length radiator made up of the lead plates of an optical spark chamber (not triggered in this experiment), followed by a hodoscope of 2.5 radiation length thick lead-scintillator sandwich counters (SA), with pulse-height measurement. The mean pulse height of electrons in this counter was linearly proportional to their energy, having a value of five times the minimum ionization at a c.m.s. momentum of 1 GeV/c . The energy resolution of the detector was $\Delta E/E = \pm 30\%$.

The electromagnetic shower detector in Arm 2 consisted of a 0.85 radiation length thick iron plate, followed by a hodoscope of 16 scintillation counters (Z), and then by an array of 17×7 total absorption lead-glass Čerenkov counters with a thickness equivalent to 14.8 radiation lengths. The r.m.s. energy resolution of these counters was measured to be $\Delta E/E = 0.017 + 0.064/\sqrt{E}$ (E in GeV).

Each arm also contained three scintillation counter hodoscopes (H_1, H_2, H_3 , in Arm 1, and H'_1, H'_2, H'_3 , in Arm 2). Hodoscopes H_1 and H'_1 were equipped with pulse-height measuring electronics. A more detailed description of the two spectrometers and of their performance may be found elsewhere¹⁻³).

The study of the production of high mass e^+e^- pairs proceeded simultaneously with the search for single electrons previously reported³). Two independent triggers were used, namely a single electron trigger in either of the two spectrometer

arms with minimal or no triggering requirement from the other arm. For each trigger, all the information from both arms was recorded on magnetic tape. The Arm 1 trigger consisted of a coincidence $H_1 \cdot H_2 \cdot H_3 \cdot C \cdot SA$. For approximately half the experiment, $H_1' \cdot H_2' \cdot H_3'$, the scintillators in Arm 2, were also required. The Arm 2 trigger, which was also the trigger for the single electron search³⁾, required $H_1' \cdot H_2' \cdot H_3' \cdot C'$ in coincidence with an energy deposition in the lead-glass array exceeding a given threshold. During the data taking, two nominal threshold values were used, corresponding to about 1.0 and 1.2 GeV in the centre-of-mass system.

The two triggers used had slightly different properties, which complemented each other. The Arm 2 trigger had the advantage of enabling the e^+e^- pair measurement to be normalized to the single electron data; but had the disadvantage of an energy threshold in the trigger. The Arm 1 trigger had no threshold bias and thus had a wider mass acceptance than the Arm 2 trigger; but the poorer resolution of the electromagnetic shower detector in Arm 1 gave less of a constraint in separating electrons from pions.

In the off-line analysis, those events were selected in which two, or more, charged particles were present, originating from a common vertex and traversing the two spectrometer arms, at least one in each arm. Charged particle tracks were required to set the bits of all scintillation counters through which their trajectories passed, consistent with the triggering conditions.

The main sources of background which could simulate electrons in either arm were: i) photons from π^0 decay, converting in the walls of the ISR vacuum chamber or the H_1 or H_1' hodoscopes; ii) π^0 Dalitz decays; and iii) charged hadrons satisfying the electromagnetic shower requirements described below, in association with a signal from the appropriate C or C' counter cell.

In order to select electron-pair events, various cuts were applied: i) both tracks had to set the bits corresponding to the appropriate C and C' counter cells traversed; ii) the pulse heights in the H_1 and H_1' hodoscopes had to be between 0.5 and 1.5 times minimum ionization, corresponding to a single particle (this greatly suppressed those electrons due to photon conversions and Dalitz decays); iii) both tracks had to have sparks in the spark chambers located between the ISR vacuum chamber and hodoscopes H_1 and H_1' (this requirement eliminated electrons due to photon conversions in H_1 and H_1'); iv) the track in Arm 1 had to give a pulse in the appropriate SA counter, corresponding to at least two times minimum ionization; and v) the track in Arm 2 had to deposit in the lead-glass array a total energy equal, within $\pm 30\%$, to its momentum, as determined using the magnet.

In order to achieve constant electron detection efficiencies, the centre-of-mass momenta in Arm 1 and Arm 2 were required to be larger than a certain value, which depended on the trigger. The net effect of all these cuts produced detection efficiencies for electrons within the geometrical apertures of Arm 1 and Arm 2 of $84 \pm 4\%$ and $45 \pm 5\%$, respectively; and the corresponding hadron rejections obtained were $> 3 \times 10^3$ and 2.0×10^4 . The values of the angular apertures and momentum cuts used are given in Table 1.

Data were taken at four values of the total centre-of-mass energy, $\sqrt{s} = 30.6, 44.8, 52.7, \text{ and } 62.4 \text{ GeV}$. For an integrated luminosity of $1.79 \times 10^{36} \text{ cm}^{-2}$, distributed among the four \sqrt{s} values in the proportion of 16%, 27%, 50% and 7% respectively, a total of 11 electron-pair events were found. It is important to note that in all of these events the two electrons had opposite charges. No e^+e^+ or e^-e^- pairs were found.

Three types of background events could contribute to the 11 e^+e^- pairs observed in the experiment: a single electron candidate in Arm 2 in combination with either i) a charged hadron or ii) a Dalitz decay or photon conversion in Arm 1, which are mis-identified as electrons, and iii) a real single electron in Arm 1 in combination with an Arm 2 single electron candidate which is not a real electron.

All three types of background can be directly determined by using the Arm 2 trigger. For the integrated luminosity given above, a total of 3190 single electron candidates were detected, which satisfied the Arm 2 trigger and cuts. In 22 of these events, a charged particle having a c.m.s. momentum above 1 GeV/c was also detected in Arm 1. These 22 particles were identified as 13 charged hadrons (no C signal, SA ignored), and 9 electrons^{*)}. It is known^{1,2)} that the charged hadron rejection in Arm 1 is $> 3 \times 10^3$, and the rejection against Dalitz decays and photon conversions is 4.5×10^4 , normalized to charged hadrons. Thus the contributions from backgrounds (i) and (ii) turn out to be $< 4.3 \times 10^{-3}$ and 0.3×10^{-3} events, respectively. It is also known from our single electron search^{3,4)} that the single electron candidates satisfying the Arm 2 trigger and cuts consist of 53% directly produced electrons, 37% mis-identified charged hadrons^{**)}, and 10% electrons from photon conversions and Dalitz decays. For Arm 1, it is assumed that the natural particle composition [e/π ratio³⁻⁵⁾ = 1.2×10^{-4}] would be observed, if it were not for the Arm 2 trigger. Thus, the contribution from background (iii) becomes 0.7×10^{-3} events, resulting in an over-all background contribution of $(6.5 \pm 2.0) \times 10^{-3}$ events to the 11 e^+e^- pairs observed in this experiment. It

*) These 9 events, together with 2 other events obtained only with the Arm 1 trigger, comprise the 11 e^+e^- pairs observed in this experiment.

***) The C' pulse-height cut used in Ref. 3 is not applied here, resulting in a higher hadron contamination.

must be stressed that all types of background would generate an equal number of same-charge and opposite-charge events, while the observed pairs all have opposite charges. It can thus be concluded that the 11 e^+e^- pairs are genuine and correspond to the occurrence of reaction (1).

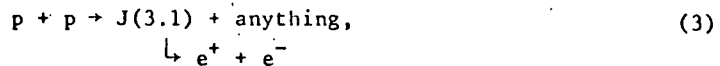
The invariant mass of each pair was calculated using the momenta of the particles as measured in the magnetic spectrometers. The distribution of invariant masses of the 11 events is shown in Fig. 2 and the events are listed in Table 2. The e^+e^- invariant mass resolution was determined from the known measuring errors on momenta. The resolution function was found to be Gaussian with a standard deviation of 3.5% over the mass interval from 2.5 to 4.0 GeV/c².

The geometrical acceptance of the apparatus for reaction (1) as a function of $M(e^+e^-)$ was estimated by a Monte Carlo calculation. A distribution of the form

$$E \frac{d^3\sigma}{dp^3} = \frac{d^2\sigma}{2\pi p_T^* dp_T^* dy} \propto e^{-bp_T^*} \quad (2)$$

was assumed for reaction (1), where p_T^* is the transverse momentum and y the rapidity of the e^+e^- pair in the centre-of-mass system. The flat rapidity distribution of Eq. (2), within the acceptance of the apparatus, is suggested by the data (Fig. 3). The value of the geometrical acceptance depends strongly on $\langle p_T^* \rangle = 2/b$ because events with large p_T^* become non-collinear in azimuth and miss the detector. It was determined from the observed events that $\langle p_T^* \rangle \geq 0.67$ GeV/c to 85% confidence, so that the value $b = 3$ GeV⁻¹ was used to compute the acceptance. Finally the decay angular distribution was taken to be isotropic in the rest system of the pair^{*)}.

The shape of the apparatus acceptance versus $M(e^+e^-)$ is shown in Fig. 2 for both the Arm 1 and Arm 2 triggers. The Arm 2 trigger was active for the full luminosity of the experiment and the Arm 1 trigger for 90% of the luminosity. Hence, the absence of events observed between 2.20 and 2.90 GeV/c² strongly suggests that the nine events clustered around $M(e^+e^-) = 3.1$ GeV/c² in Fig. 2 result from the reaction



where J(3.1) is the narrow particle recently discovered at BNL⁶⁾ and SPEAR⁷⁾. These nine events have a mean mass of 3.075 ± 0.037 GeV/c² and a standard deviation of 0.11 GeV/c². No firm conclusion can be reached on the origin of the two events at higher invariant mass values, although they are consistent, within the mass resolution, with the e^+e^- decay of the $\psi(3.7)$ particle⁸⁾.

*) Decay angular distributions of the form $\sin^2 \theta$ or $1 + \cos^2 \theta$ would change the acceptance by a factor of 1.13 and 0.93, respectively.

Using the acceptance calculations discussed above, it is possible to obtain an estimate of the cross-section for reaction (3) at ISR energies. In this experiment, reaction (3) is only observed in the J rapidity interval between -0.32 and +0.32. The cross-section result is expressed in the form

$$B_{ee} \times \left. \frac{d\sigma}{dy} \right|_{y=0} (p + p \rightarrow J + \text{anything}) = (7.5 \pm 2.5) \times 10^{-33} \text{ cm}^2$$

averaged over this interval, where B_{ee} is the branching ratio for the decay mode $J(3.1) \rightarrow e^+ e^-$. It should be noted that a change from $\langle p_T^* \rangle = 0.67$ to higher values in the acceptance calculation would cause the above cross-section to increase. (See Table 3).

The value of the cross-section for reaction (3) at ISR energies is two orders of magnitude higher than the corresponding value quoted at BNL energies⁶⁾. A comparison with the Fermilab⁹⁾ measurement is more difficult since the experiments are done in disjoint regions of rapidity.

The Fermilab results were converted to differential cross-sections in their variable^{*} x by using their quoted x dependence, $\exp(-10 x)$. The cross-sections were then transformed to be differential in rapidity y , by using the Jacobian $d\sigma/dy \approx x d\sigma/dx$. As shown in Figure 4, the two experiments are in good agreement. Also note that the p_T^* distribution quoted at Fermilab corresponds to $\langle p_T^* \rangle = 0.707$. If the rapidity distribution of Fig. 4 is taken seriously, then the differential cross-section $B_{ee} \times d\sigma/dy|_{y=0}$ given above can be converted into the total cross-section, $B_{ee} \times \sigma_{tot}$, for reaction³⁾ by multiplying by a factor of 1.6.

An interesting question is whether reaction (3) is sufficient to account for the single lepton signal observed in hadron collisions^{3,5,10)}. The answer is most simply obtained by using the acceptance calculation discussed above, to predict absolutely the single electron transverse momentum distribution and the ratio of electron pairs to single electrons to be observed in this experiment (Arm 2 trigger), if all the single electrons were due to reaction (3). An additional assumption used is that Eq. (2) is flat in rapidity for $|y| \leq 0.8$. The result is a predicted pairs-to-singles ratio of 5.3% for $\langle p_T^* \rangle = 0.67$, and 3.1% for $\langle p_T^* \rangle = 1.0$ GeV/c. The observed ratio is $(0.53 \pm 0.17)\%$, which shows that there are roughly five to ten times more single electrons observed than can be explained by reaction (3). For larger values of $\langle p_T^* \rangle$, the predicted pairs-to-singles ratios are in closer agreement with the observed value, but the transverse momentum distributions of the single leptons are in disagreement with those observed^{3-5,10)} (Fig. 5). The origin of the single leptons is still an open question.

*) Note that this is not the Feynman x but is the ratio of the outgoing momentum of the $J(3.1)$ to the momentum of the incident neutron, in the laboratory system.

We wish to thank Professors R.L. Cool and L.M. Lederman for their continuous interest and support; R. Boulhot, R. Gros, M.A. Huber, M. Lemoine and G. Sicher for technical help; and the ISR crew for the excellent performance of the machine.

REFERENCES

- 1) M. Banner et al., Phys. Letters 44B, 537 (1973).
- 2) J. Gresser, Thesis, CRN/HE 74-10 (Centre de recherches nucléaires de Strasbourg, France, 1974).
- 3) F.W. Büsler et al., Phys. Letters 53B, 212 (1974).
- 4) S.N. White, Thesis (Columbia University, NY, 1975);
F.W. Büsler et al., High transverse momentum electrons at the CERN ISR
(submitted to this conference).
- 5) J.A. Appel et al., Phys. Rev. Letters 33, 722 (1974).
- 6) J.J. Aubert et al., Phys. Rev. Letters 33, 1404 (1974).
- 7) J.E. Augustin et al., Phys. Rev. Letters 33, 1406 (1974).
- 8) G.S. Abrams et al., Phys. Rev. Letters 33, 1453 (1974).
- 9) B. Knapp et al., Phys. Rev. Letters 34, 1044 (1975).
- 10) J.P. Boymond et al., Phys. Rev. Letters 33, 112 (1974).

Table 1

Angular apertures and kinematic cuts for the two spectrometers in the centre-of-mass system for the two triggers

Trigger	Spectrometer arm	θ^* (degrees)	ϕ^* (degrees)	$\Delta\Omega^*$ (sr)	p_T^* cut (GeV/c)
Arm 1	1	90 ± 13.3	0 ± 4.7	0.075	≥ 1.0
	2	90 ± 22.5	180 ± 7.2	0.192	≥ 1.0
Arm 2	1	90 ± 13.3	0 ± 4.9	0.078	≥ 1.0
	2	90 ± 22.5	180 ± 7.2	0.192	≥ 1.3

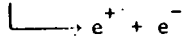
Table 2

Kinematical parameters for the observed e^+e^- pairs

\sqrt{s} (GeV)	$M(e^+e^-)$ (GeV/c ²)	p_T^* (GeV/c)	y
44.8	2.93	0.88	-0.165
52.7	2.99	0.78	-0.033
52.7	3.00	0.20	0.239
44.8	3.02	0.33	0.191
44.8	3.07	0.72	-0.007
52.7	3.07	0.30	0.157
30.5	3.12	0.32	0.318
44.8	3.18	0.33	0.095
52.7	3.29	1.43	-0.001
52.7	3.46	1.18	0.193
52.7	3.79	0.36	0.121

Table 3

Differential cross-section for the reaction
 $p + p \rightarrow J(3.1) + \text{anything}$



for various values of assumed $\langle p_T^* \rangle_J$

$\langle p_T^* \rangle_J$ (GeV/c)	$B_{ee} \times \frac{d\sigma}{dy} (p + p \rightarrow J + \text{anything})$ (cm^2)
0.67	$(7.5 \pm 2.5) \times 10^{-33}$
1.0	$(1.2 \pm 0.4) \times 10^{-32}$
1.5	$(2.1 \pm 0.7) \times 10^{-32}$
2.0	$(3.2 \pm 1.1) \times 10^{-32}$

Figure captions

- Fig. 1 : Plan view of the apparatus.
- Fig. 2 : Invariant mass distribution for the observed e^+e^- pairs. The curves represent the shapes of the acceptance, as a function of the e^+e^- invariant mass value, for the Arm 1 and Arm 2 triggers, respectively.
- Fig. 3 : Rapidity distribution for the observed e^+e^- pairs. The curve represents the shape of the apparatus acceptance, which is the same for both triggers.
- Fig. 4 : Differential cross-sections versus rapidity for the production of J(3.1) in nucleon-nucleon collisions. The results of reference 9 have been transformed as explained in the text.
- Fig. 5 : Absolute prediction of single electron spectrum from reaction (3) using the cross-sections given in Table 3. The data is from Ref. 4.

PLAN VIEW OF APPARATUS

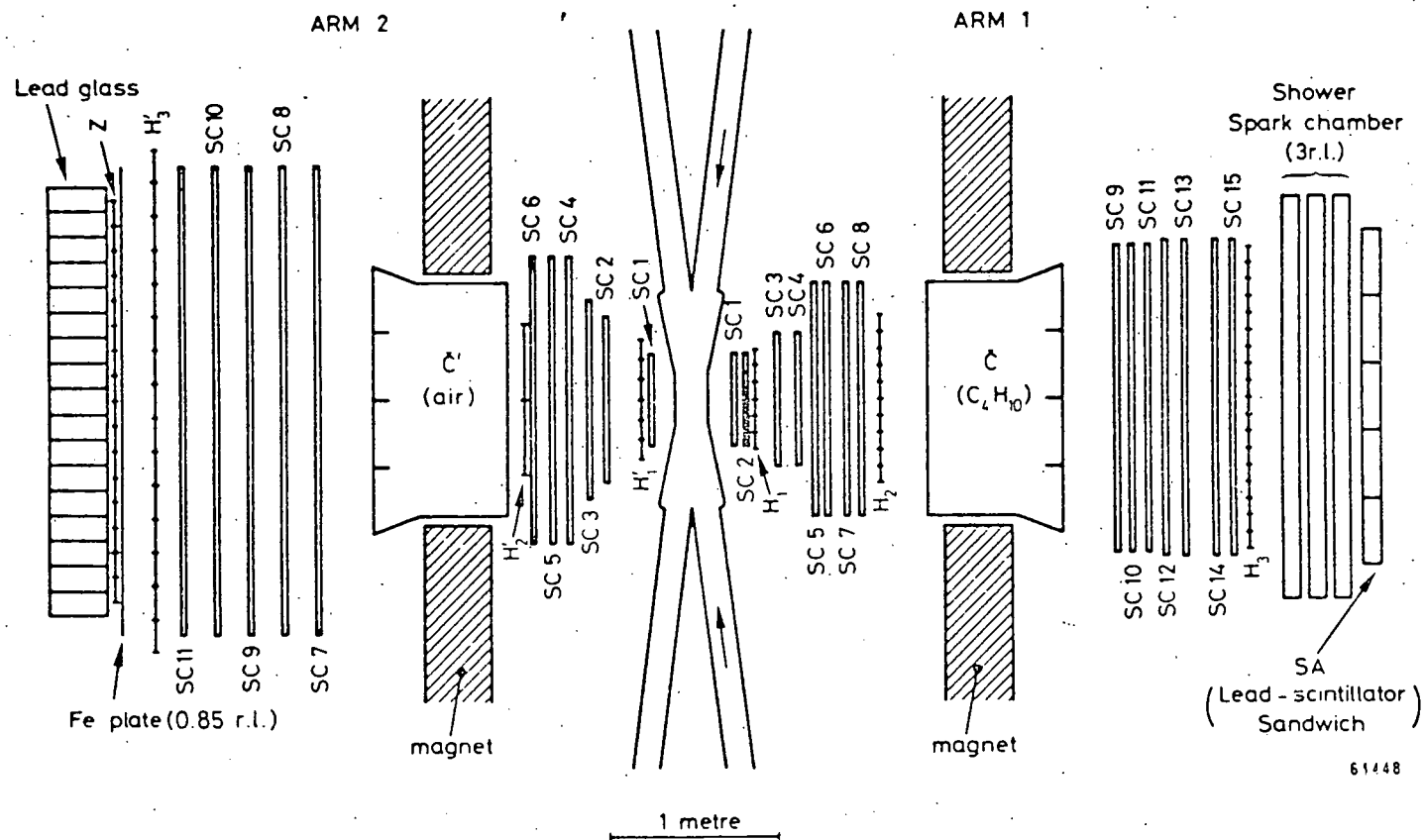


Fig. 1

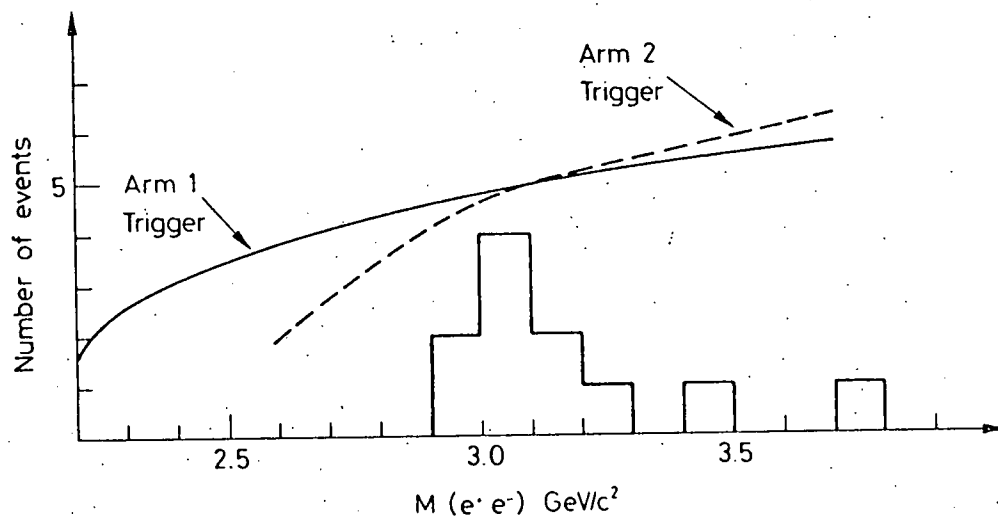


Fig. 2

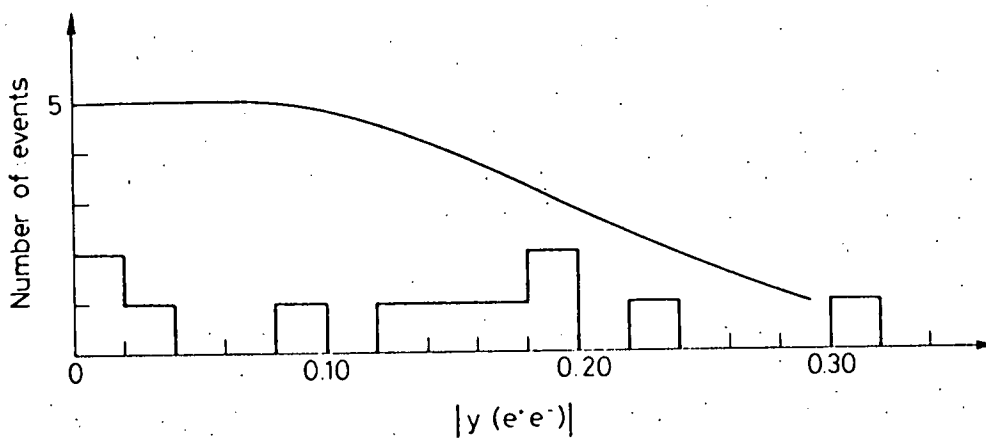


Fig. 3

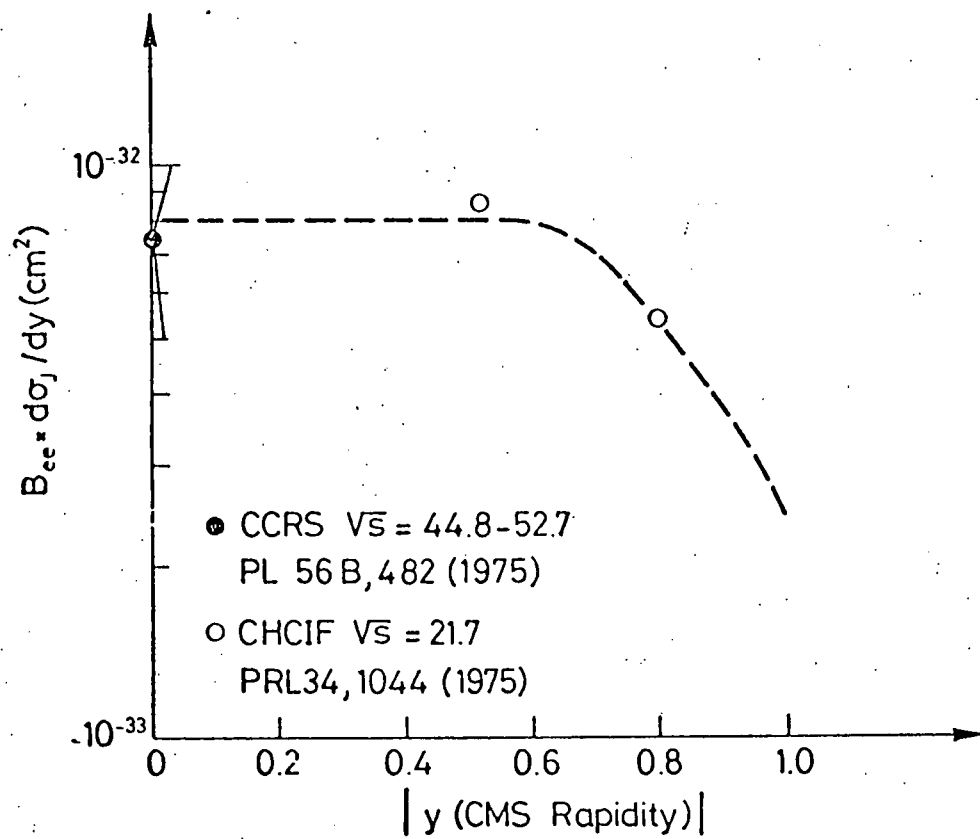


Fig. 4

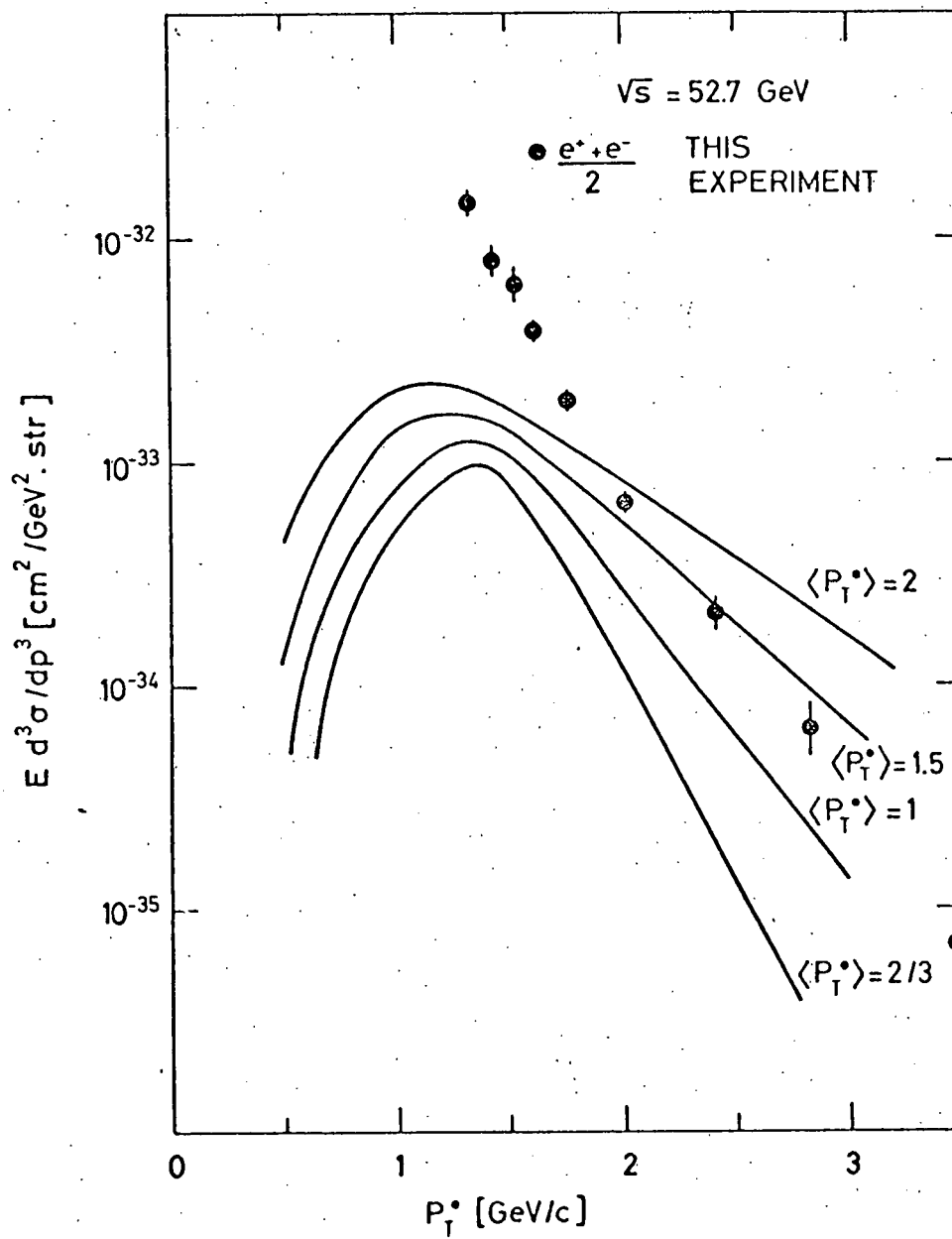


Fig. 5